Title:

Ear pinnae in a neotropical katydid function as ultrasound guides for bat call detection

Running title:

Tympanal pinnae in katydids

Christian Pulver[1], Emine Celiker[1], Charlie Woodrow[1], Inga Geipel[2,3,4], Carl Soulsbury[1], Darron A. Cullen[1], Daniel Veitch[1] & Fernando Montealegre-Z[1,5]

[1]University of Lincoln, School of Life Sciences, Joseph Banks Laboratories, Green Lane, Lincoln, UK, LN6 7DL

[2]Smithsonian Tropical Research Institute, Apartado 0843-03092, Balboa, Panama.

[3]CoSys Lab, Faculty of Applied Engineering, University of Antwerp, 2020 Antwerpen, Belgium

[4]Flanders Make Strategic Research Centre, 3920 Lommel, Belgium

[5]Lead contact

*Correspondence: fmontealegrez@lincoln.ac.uk

eceliker@lincoln.ac.uk

Keywords: Orthoptera, bioacoustics, ultrasound hearing, bat predation, cuticular pinnae, pressure – time difference receiver

Abstract

Early predator detection is a key component of the predator-prey arms race, and has driven the evolution of multiple animal hearing systems. Katydids (Insecta) have a sophisticated ear consisting of paired tympana on each foreleg that receive sound externally and internally, creating a pressure-time difference receiver system capable of sensitive and accurate directional hearing, despite the katydid's small size. Some katydid species have pinnae of unknown function, which form cavities around the outer tympanal surfaces and have been hypothesised to influence the external sound paths. Combining experimental biophysics and numerical modelling on 3D ear geometries, we investigated pinnae function in the katydid *Copiphora gorgonensis*. Pinnae induced large sound-pressure gains that enhanced sound detection at high ultrasonic frequencies (> 60 kHz), matching the echolocation range of their nocturnal insectivorous predators. Comparing pinnal mechanics of sympatric katydid species supported these findings, and suggests that pinnae evolved primarily for enhanced predator detection.

Introduction

Throughout the animal kingdom, the need to localize sound signals, both to detect conspecifics and to avoid predation, is a major evolutionary selection pressure. As a result, vastly different species have convergently evolved mechanisms of hearing to fulfil similar functions[1–3], and hearing organs have evolved in closely related taxonomic groups many times independently[1,4,5]. To determine the location of a sound source, an animal with two ears will utilize interaural time and amplitude differences. Such binaural auditory systems must satisfy three requirements to function: (1) the distance between each ear must be sufficient to produce recognisable differences in sound arrival time, (2) the ears must be separated by a body which

is large enough to attenuate sound between them, (3) the ears must be neurologically coupled in order to calculate time and amplitude differences[6,7]. However, small animals such as insects are too small to exploit diffractive effects of sound on their bodies to perceive minute differences in sound delays and intensities[8]. Katydids (Orthoptera: Tettigoniidae), a group with ~8,000 species[9] , have overcome this problem by evolving independently functioning ears in their forelegs[10], thereby increasing the interaural distance. Many species have also evolved the ability to produce and detect ultrasonic frequencies[11], meaning that the resulting distance between the ears provides sufficient spatial separation to exceed the shorter wavelengths of incoming conspecific sounds[2]. Each tettigoniid ear receives sound directly at the external tympanal surface, but also internally in a process similar to that of the mammalian ear. In this internal process, sound enters an air-filled ear canal (EC, also called acoustic trachea) through a specialised opening in the prothorax known as the acoustic spiracle[12]. The EC's narrowing, exponential horn shape amplifies the sound signals[13–20] and reduces propagation velocity[13,14,20], and leads this decelerated sound signal through the thorax and foreleg to the internal tympanal surface. The combined internal and external inputs means that the tettigoniid ear functions as a pressure – time difference receiver[2,13–21], unlike the mammalian ear which functions as a single input pressure receiver via the EC.

At the external auditory input, some tettigoniids also possess cuticular pinnae (also referred to as folds, flaps or tympanal covers) partially enclosing their tympana (Fig. 1a-c). Early observations by Autrum suggested that the cuticular pinnae aided the insect to determine the direction of sound, effectively acting as a sound guide[22,23]. The prominence of cuticular pinnae present in a variety of Pseudophyllinae and Conocephalinae species (see examples in the Supplementary Fig. S1a and S1c-k) generated more interest in these observations. Morphologies of cuticular pinnae vary greatly between species, and were originally categorized in a phylogenetic context[10]. A dual functioning auditory system in the tettigoniid *Mygalopsis*

marki was proposed to explain differences in the auditory morphologies in spiracle size and tympanal pinnae in which the external tympanal ports appears to function as omnidirectional receivers and the EC combined with the spiracle operate as a highly sensitive non-directional receiver[24]. These findings were corroborated in *Hemisaga* sp. where it demonstrated increased acoustic sensitivity at the external tympanal port (through blocking the entrances or slits from here forth) [25]. A dual channel system consisting of the EC and spiracle serve for the detection of predators, whilst the external tympanal ports are used for detecting conspecific communication signals[25]. Studies of ultrasonic rainforest Pseudophyllinae provided more evidence of principal sound reception for conspecific communication using the external tympanal port as a consequence of exceptionally small spiracle sizes[26]. It was reported that diffraction of very short wavelengths along the tympanal slits contributed to directional orientation in rainforest katydids[26].

Despite these findings, the role of cuticular pinnae has been subject to considerable debate in the literature. Before experimental evidence of the dual port system in katydids was published[13,20], attention was given to the EC as the main port for sound capture[18,27–31]. Moreover, it has been argued that the size of the ear is considerably smaller than the wavelengths of most carrier frequencies of described insects known at the time, and therefore the sound pressure field around the ear would be constant and yield no directional cues[28]. In other words, sound accessing the external tympanal port is not related to the direction of incidence, and tympanal pinnae are merely protective features sheltering the fragile tympanum. However, recent research showed that quieter, low amplitude sound waves acting on the external tympanal membrane (without gain from the EC) of the neotropical katydid *Copiphora gorgonensis* (Tettigoniidae: Copiphorini) do cause vibrations of significant amplitude in the inner ear[32]. Therefore, even these very weak vibrations are mechanically transduced. The external sound arrives 60-80 µs before its amplified form of self on the internal tympanal

surface via EC, and this significant phase delay forms the basis of the pressure – time difference receiver definition[13,14]. In katydids with cuticular pinnae surrounding the tympana, evidence suggests that the insect can use both ports, but how the external port contributes to directionality remains unknown[33].

Here, we investigate the role of cuticular pinnae using the neotropical katydid *Copiphora gorgonensis*, a species endemic to Gorgona, an island in the Pacific Ocean off the western coast of Colombia[34]. *Copiphora gorgonensis* has become a model species for hearing studies due to the transparency of the cuticle which facilitates non-invasive, real-time measurements of the inner ear[32,35]. We integrated experimental biophysical measurements based on micro – scanning laser Doppler vibrometry (LDV) and micro-computed tomography to simulate the function of the cuticular pinnae and how they contribute to auditory orientation in this katydid. The coupling of these approaches were applied to 3-dimensional (3D) print models of the ear, and scaled experiments were performed to validate the simulations. We investigated if: (1) the direction of incidence of the sound stimulus, presented by a loudspeaker, is a function of the sound wave directly accessing the tympana through the slits; (2) the tympanal cavities produce sound pressure gains that act externally on the tympana; (3) tuning properties of the pinnal cavities are a result of pinnal geometry and can be predicted by the volume and/or entrance size of the cavity.

Based on Autrum's original observations, we hypothesized that tympanal pinnae function as ultrasonic guides by pinnae forming exceptionally small resonant cavities. Further, we hypothesized that these cavities act as Helmholtz-like resonators able to capture and amplify diminishing ultra-high frequency waves.

Results

Time domain response of the external tympanal port

We investigated the role of tympanal pinnae in sound capture by testing how the direction of incidence of the sound stimulus presented by the loudspeaker induced tympanal displacements at three frequencies (23, 40 and 60 kHz) with the cuticular pinnae intact and later ablated. Frequencies above 60 kHz were not tested provided the limitations of experimental equipment (see methods for *vibration measurements*). A total of 2,736 measurements were performed on 13 ears (1,512 measurements for male specimens; 1,224 for female specimens). For time to sound arrival, we found a significant interaction between the presence of cuticular pinnae with angle of incidence and with frequency (Supplementary Table S1). Post hoc analysis showed the presence of pinnae significantly slowed the time of arrival at 23 kHz (t-ratio = -11.15, $P < 0.001$) and 40 kHz (t-ratio = -7.43, $P < 0.001$), but not at 60 kHz (t-ratio = -1.86, $P = 0.063$; Fig. 2b). The effect of tympanum on time of arrival and displacement amplitudes was found to be significant (Supplementary Table S1).

For displacement amplitude, there was a significant interaction between the presence of pinnae and frequency (Supplementary Table S1). Post hoc analysis showed greatest displacement amplitudes at 23 kHz with the pinnae ablated (t-ratio = 3.20, $P < 0.001$; Fig. 2c), which demonstrates that pinnae do not enhance auditory perception of the carrier frequency in *C. gorgonensis*, and that the tympanum achieves this displacement by resonance (see[13,35]). There were no differences at either 40 kHz (t-ratio = 0.84, $P = 0.399$; Fig. 2c) and 60 kHz (t-ratio = -0.61, $P=0.540$; Fig. 2c). We also found a significant interaction between the presence of cuticular pinnae with angle of incidence showing the impact of pinnae in increasing arrival time as the sound source rotates opposite the ear (Supplementary Table S1). Responses were strongest for sound presented perpendicular to each respective slit cavity with the area of the cuticular septum bifurcating the cavities, also referred as “point zero,” obtaining the lowest displacement amplitudes with the pinnae intact due to cuticle obstructing the response of the

tympanal membrane . Contrarily, point zero showed the greatest displacement amplitude with the pinnae ablated with incident angles on either side of point zero showing a gradual subdued response to the stimulus.

Anatomical measurements of the external tympanal port

The anatomical features of the ear were measured to predict resonance and compare intraspecific variation in pinna size. 2D measurements of the area of the pinnal opening (slit), distance between the centre of the ear (septum) and edge of the pinna (pinnal protrusion), and distance between slits (septum width) were studied using an Alicona Infinite Focus microscope (n = 8). We found that the size of the slit was not significantly different between the ATM and PTM (Wilcoxon paired rank sum test, P = 0.958). The pinnal protrusion length showed that the PTM pinnae were significantly wider than the ATM (two sample t test, $t(14) = -4.64$, $P < 0.001$).

The 3D measurements of the tympanal cavity volumes and cross section of the ears showed that the PTM cavity volume was slightly larger than the ATM volume, but insignificant (Wilcoxon paired rank sum test, P = 0.958). The mean cross-sectional width of the ear was 1.143 mm ± 0.353 (n = 8).

Tympanal cavity resonance calculations

We used the 2D (slit area) and 3D measurements (cavity volume) to estimate resonance of the tympanal cavities (Supplementary Table S2). This was calculated with the assumption that the slit openings are a perfect circle (to determine radius) and the cavity acts as a cylindrical tube using a neckless Helmholtz resonance equation. Here, c is speed of sound in air (343 m s^{-1}), S

is cross-sectional area of the opening with radius r, 1.85 is the correction length of the neck and V denotes the volume of the resonator / cavity[36].

$$f(h) = \frac{c}{2\pi}\sqrt{\frac{1.85r}{V}}$$

The pinnal cavities (n = 8) showed a neckless Helmholtz resonance of 94.280 ± 3.532 kHz for the ATM and 91.694 ± 3.929 kHz for the PTM (Wilcoxon paired rank sum test, P = 0.093).

3D printed model time and frequency domain measurements

3D printed scaled models of the ear were subjected to acoustic experimentation to measure gain and resonance. 3D ears were printed at a scale of 1:11.43 and stimuli was scaled by the same factor for pure tones (2.01 kHz for 23 kHz, 3.50 kHz for 40 kHz, 5.25 kHz for 60 kHz, and 9.63 kHz for 110 kHz) and for broadband (2-15 kHz for 11.5-170 kHz). The interaction between pinnae and frequency significantly affected sound pressure (dB), whilst tympanum did not (Supplementary Table S1). Across all frequencies, the presence of pinnae increased sound pressure, but differences were greatest at higher frequencies (23 kHz: t-ratio = -2.54, P = 0.014; 40 kHz: t-ratio = -8.69, P < 0.001; 60 kHz t-ratio = -15.66, P < 0.001; 110 kHz t-ratio = 41.70, P < 0.001; Fig. 3a). More specifically, the greatest pressure gains were detected at 104.65 kHz for both the ATM (24.19 dB) and PTM (27.68 dB) with the pinnae intact. With the pinnae ablated, the greatest pressure gain was found to be 97.98 kHz for both the ATM (8.04 dB) and PTM (7.81 dB).

Numerical results

Using real 3D geometries of each experimental ear, we used Finite Element Analysis (FEA) to simulate sound pressure gains at frequencies exceeding the experimental limitations on living specimens. For sound pressure measurements there was a significant interaction between the presence of pinnae and frequency (Supplementary Table S1). At 23 kHz ears without pinnae had significantly higher sound pressures (t-ratio = 3.45, $P < 0.001$), but the effect was reversed at 40 kHz (t-ratio = -5.94, $P < 0.001$) and 60 kHz (t-ratio = -28.52, $P < 0.001$), with differences increasing as frequency increased (Fig. 2d). There was no effect of angle of sound incidence or tympanum on sound pressures (Supplementary Table S1).

Simulated sound pressure gains (Figs. 4c and 4d), and their distribution maps (Fig. 4a and 4b) showed the greatest sound pressure gain at a mean value of ~118 kHz (ATM mean 121 kHz, PTM mean 115 kHz), and such gains were reduced or lost entirely when the pinnae were removed (Supplementary Table S1; Fig. 4d).

The effects of angle, pinnae, tympanum, interaction of angle and pinnae, and the interaction of pinnae and frequency were not significant on arrival times (Fig. 2e).

Behavioral and tympanal response to broadband stimulation

For broad tympanal responses, we exposed seven specimens to broadband periodic chirps stimulation in the range 20-120 kHz in a free sound field and recorded the vibration of both ATM and PTM, of the two ears using a micro-scanning laser Doppler vibrometer. Pinnae induced sound pressure produced a relatively stable response (measured as velocity per sound pressure) of the tympanal membranes between 20-70 kHz, however above 80 kHz the tympana response increased dramatically with ultrasonic resonant peaks at~107 kHz for the ATM and ~109 kHz for the PTM (Fig. 5a).

Behavioural audiograms were obtained from nine tethered females walking on a treadmill. Audiograms were obtained with stimuli in the range 20-120 kHz, as this species is entirely

ultrasonic (males call with a 23 kHz pure tone). Audiograms show that the startle response of females decline sharply for stimuli between 20 kHz and 35 kHz, however, response remains essentially constant at higher frequencies (Table S3; Fig. 5b).

Discussion

To understand the function of cuticular pinnae of katydid ears, we conducted acoustic experiments on living specimens and used micro-CT to produce images for numerical modelling using accurate ear geometries, and to print 3D scaled ears for additional acoustic experiments. In all our experiments, pinnae had a significant effect on the sound reception at the tympana. Pinnae significantly enhanced cavity-induced pressure gains in live specimens at 60 kHz (the maximum frequency achieved with the experimental platform for living specimens). Further, the extent of the pinnal contribution to tympanal displacement amplitude depended on the incident angle of the sound source at tested frequencies $\leq$ 60 kHz. The tympana of *C. gorgonensis* naturally resonates at ca 23 kHz, which shows high sensitivity to the dominant frequency of the male calling song[34,37]. This was also observed in our experimental results, irrespective of pinnal presence or absence. At ultrasonic frequencies, the pinnae-enclosed tympanal membrane of *C. gorgonensis* show strong mechanical vibrations induced by the resonances of the tympanal cavities (Fig. 5a). This suggests that tympanal pinnae enhance sound pressure and sensitivity to high frequencies. It was previously demonstrated that even minuscule tympanal displacements in *C. gorgonensis* create large displacement of the *crista acustica* (CA)[32]. Tympanal displacements are nearly duplicated in the CA as the effect of the lever action imposed by the vibration of the tympanum measured though transparent cuticle[35] . Comparable findings can be inferred from LDV experiments on the katydid *Mecopoda elongata,* with its CA exposed[38]. Insect mechanosensory auditory

neurons are capable of detecting exquisitely small mechanical displacements, down to 100 pm[39], close to the theoretical limits of sensitivity[40]. Therefore, the sound pressure gain induced by the tympanal pinnae at ultrasonic frequencies (> 60 kHz; Fig. 3a and Fig. 5a) should produce sufficient tympanal displacement without EC amplification to create a response in the auditory receptors. Recordings from the T-cell in *Tettigonia viridissima* (another katydid with tympanal pinnae) show a broad sensitivity in the range 5-90 kHz[41].

As a result of probe-speaker limitations and reflections from the specialised platform in our live time domain experiments, we were unable to test frequencies above 60 kHz. We compensated by performing numerical simulations on 3D computer geometries of experimental ears to predict pressure gains; 3D printing ear models to confirm resonance and pressure gain; and recording experimental free field vibrating tympana. Our numerical simulations predicted sound pressure gains in the frequency range of 50 – 150 kHz with mean resonant frequencies of 115 kHz and 121 kHz in the PTM and ATM cavities, respectively (Fig. 4c). Between 50–60 kHz, detectable pressure gains inside the cavity started to act along the external tympanal membrane with the best gain of about 23 dB found at resonant frequencies. We did not compare the tympanal response between the experimental and numerical data directly, due to the simplifying assumption in the numerical models that the tympana are composed of homogeneous material. In reality, the tympanal layer is composed of materially different layers where the external surface has more chitinous, sclerotized layers extending from the tympanal plate to the membrane, while the internal membrane is composed of elastic, tracheal derived material. To overcome this, we measured tympanal vibrations to extreme ultrasound in free field conditions to validate both the numerical and 3D print model results.

To test the influence of pinna geometry alone on these ultrasonic gains, we 3D printed ears and scaled the sound stimuli to match the ear size. The mean resonance of the 3D printed models was found to be ~105 kHz (Fig. 4e). Differences between the numerical and 3D print models

results can be attributed to the material properties (Young's modulus of printing resin) incorporated for the tympana in the models. When we simulated these material properties of the 3D ears, the resonant frequencies dropped to ~111 kHz (ATM 112.5 kHz, PTM 109.5 kHz; Supplementary Fig. S2) which is close to the high frequency resonance of the tympana when the pinnae are intact (107.5 kHz; Fig. 5a). Without the pinnae, pressure gains were dramatically reduced in the simulations. Additionally, a slight resonance was found in both the numerical simulations and 3D print models caused by the incomplete ablation of the pinnal structures (Figs. 3d and 3f).

Ultrasound guides in insects

Pinnae-covered tympanal ears are also found in some prominent moths (Notodontidae), with eardrums mechanically tuned to detect the high frequencies used by hunting bats[42]. Cup-like pinnae from the metathorax are suggested to enhance the reflection of sounds onto the tympanic membrane [44]. With the pinnae ablated, these moths entirely lost the ability to localise sound at all frequencies[43]. Therefore, katydids and certain moths seem to have independently evolved pinnal adaptations for detecting bat ultrasounds.

High frequency singers of the katydid subfamily Pseudophyllinae generally have very small spiracles, long but narrow ECs, and tympana covered with various forms of cuticular pinnae[44]. Pseudophyllines with song frequencies greater than 50 kHz have been shown to depend more on external than internal sound reception for communicating with conspecifics[24–26,45]. The dominant port for hearing relies on the tympanal slit to spiracle size area ratio where the larger opening dictates principal auditory input in ultrasonic hearing rainforest pseudophyllines [26]. In *C. gorgonensis*, the spiracle area is large, naturally open on average three times larger than the total area of the tympanal slit (1 mm^2 : 0.3 mm^2) which is inversely related to the scale of

pseudophyllines. Nevertheless, reflectance and power transmittance inside the tympanal pinnal cavities experience different acoustics dynamics than the EC. Power transmittance of ultrasonic frequencies suffer significant attenuation as a result of high reflectance of sound waves along the narrowing EC in *C. gorgonensis*[46].

By concentrating or funnelling ultrasonic sound into the tympanal cavity, the pinnae enhance ultrasonic reception of incidental sounds. The cavity induced pressure gains are the consequence of geometry of the tympanal slit in relation to the geometry and volume of the cavity (Supplementary Table S2). These imparted forces are magnified by the motion of the tympanum. The resonances afforded by the pinnal structures are evident as both the numerical and 3D print models do not include a vibrating tympanum. In *C. gorgonensis*, irrespective of incident sound pressure magnitude, the cavities provide a consistent pressure gain of at least 16 dB within the frequency range 100 – 120 kHz (Fig. 4c). This is in contrast to tympanate moths that depend on the incident sound intensity for mechanical tuning of high frequency bat calls[42,43,47] to produce gains up to 16 dB[43].

Though the slit openings to both cavities are perceptively indistinguishable and statistically insignificant to each other, the ATM slit opening is slightly larger than that of the PTM, but the PTM has a larger cavity volume. These minuscule discrepancies cause differences in pressure gains and resonances between both sides. In *C. gorgonensis*, the PTM pinnal structure is approximately 13% wider than the ATM. This increases the micro-acoustical diffraction of ultrasonic frequencies entering the PTM cavity. Similar pinnal asymmetries were observed in the katydid *Oxyecous lesnei* but the ATM structure was much larger than the PTM which suggests that each tympanum is differentially tuned (for other examples see Fig. 1[48]; Supplementary Fig. S3)[49]. Here, we showed that the tympanal cavities and their asymmetric openings act as Helmholtz resonators at frequencies of 94.28 kHz for the ATM and 91.594 kHz for the PTM in *C. gorgonensis*. Though the simulations show a peak of 118 kHz (ATM 121

kHz, PTM 115 kHz), the Helmholtz calculation assumes the slit opening is a circle and the cavity is a solid walled sphere. Pressure distribution maps from the numerical models suggest that at 110 kHz (see Fig. 4a), the resonance of the pinnae may function in a piston motion, whereby fluctuating air movements are present at the opening of each independent cavity: an observation characteristic of Helmholtz resonance (Supplementary Materials Section 2: Video 2). Sound pressure gains inside the 3D printed model tympanal cavities and resonances closely matched the simulated numerical models (Fig. 4c and 4e), showing a net average sound pressure gain of 16.1 dB for the ATM and 19.87 dB for the PTM at 105 kHz.

The asymmetry of the tympanal cavities have an acoustic function. Our results show that pinnae cause intra-aural time differences and oscillation phase shifts at ultrasonic frequencies between vibrations in the ATM and PTM (Fig. 2a). This contributes to differences of intensity and arrival of sound that induce pressure gains of ultrasonic frequencies (Fig. 4c and Fig. 5a). Differential tympanal mechanical responses have also been found in the pinnae possessing paleotropical katydid *Onomarchus uninotatus* where the ATM exhibits tuning to the conspecific call and the PTM's response is tuned to higher frequencies suggesting a possible use in predator detection[50]. The ATM and PTM of *C. gorgonensis* show differential responses to ultrasonic frequencies (Fig. 4c, Fig. 5a), but how these two signals are transduced in the same auditory sensilla for potential directional hearing remains unknown, as both membranes share the same CA. Not only do pinnal structures provide a long diffractive edge for sound waves, but the dorso-ventral asymmetry between the ATM and PTM pinnae. We argue that it is also possible for asymmetries within a single ear to function in the same way, including at frequencies emitted by hunting bats, however our data do not support the idea of a single ear being directional at least in the range 20-60 kHz (which include the specific calling frequency at 23 kHz). Considering that the tettigoniid ear is capable of resolving such small differences in time and intensity between the two ears [10,49], it could resolve the direction of an attacking

bat and evoke ultrasound-triggered defensive behaviour[51]. The behavioural and ecological relevance of potential directional hearing using a single ear constitutes an outstanding question and will be the subject of future studies.

In *C. gorgonensis*, the dual inputs of the spiracle and the external port (the pinnae) function as a sound pressure gain compensation system. As previously shown for *C. gorgonensis*[46], and in other species[20,44], the spiracular port and the EC with its exponential horn geometry act as a bandpass filter limited in providing pressure gains to high ultrasonic frequencies (> 50 kHz, for *C. gorgonensis*)[14,15] and designed to enhance detection of the specific carrier frequency. The effect of the EC geometry in reducing sound velocity is as much as ~20% or ca 60 µs, and coupled with the contralateral EC, collectively a total of eight inputs are possible with each causing a vibration with variable delays in four internal and four external tympanal surfaces to the same stimulus[14]. Though the reduction in velocity contributes exceptional binaural directional cues, the external port provides real-time sensitivity to exploit fading bat ultrasounds. Ear pinnae act as extreme ultrasonic guides that resonate at frequencies closer to the high frequency components at start of the echolocation sweep of common bat predators. Hence the EC might be a less efficient method of bat detection as the angle of incidence accompanied by time delays could shorten reaction times and obfuscate the localisation of the predator.

Bat detection by resonance

It has been shown that katydids form a key part of the diet of many insectivorous species in various regions of world[52–59]. However such ecological interactions have been more intensively studied in the Neotropical regions. Gorgona Island is home to over 33 bat species with many remaining undescribed and underrepresented in wildlife inventories, including least three

substrate gleaning bats of the family Phyllostomidae[60]. Neotropical katydids have evolved sophisticated auditory features as strategies for survival against substrate gleaning bats[61–65]. The habitat of *C. gorgonensis* is in cluttered vegetation of the tropical forest understory[66]. In this environment, acoustic signals are heavily attenuated which leads to significant transmission loss[41,67], but insects have evolved sophisticated receivers to perform call discrimination in these acoustically challenging environments[68]. Acoustic adaptations by katydids to evade bat predation include the use of narrow bandwidths, high carrier frequencies, and sporadic calling in order to diminish signal proliferation in the environment[61,69–71], and ergo evade eavesdropping by bats[72]. Certain adaptations are a trade-off as the katydid becomes more conspicuous and vulnerable to other predators as the communication method changes. For example, katydids that perform vibrotaxis, even tremulations can likely attract spiders, scorpions[73] and primates, as well as bats[74,75]. Likewise, bats foraging at this level also face similar acoustic shortcomings, affecting their echolocation abilities[76]. Thus, several phyllostomid substrate gleaning bats are very well adapted to listen to prey-produced sounds like rustling noises or mating calls of, e.g., male katydids[61,77]. However, at least one gleaning bat species, *Micronycteris microtis* (Phyllostomidae), uses a sophisticated echolocation strategy to discriminate the location of katydids concealed in vegetation[78,79] (Fig. 6). Despite passive acoustic defences, calling from restrictive locations and equipped with very large mandibles and sharp fastigia, katydids like *C. gorgonensis* are predated by phyllostomid bats[65].

Here we argue that the pinnal structures of the external tympanal ports of katydid ears act as sound guides providing acute ultrasonic hearing allowing the detection of echolocation calls of hunting bats and thus an additional sensory based defence in the predatory-prey arms race. The presented numerical and experimental evidence suggests that the greatest ultrasonic gain of the pinnae is at frequencies matching those falling into the frequency range of the echolocation calls of native bat species (Fig. 5). As neotropical bats approach their target, they emit short,

broadband, multi-harmonic sweeps, demodulate the frequency from higher frequencies above 135 kHz to as low 35 kHz[78,80]. In terms of predator detection, a katydid like *C. gorgonensis* has an excellent chance of detecting the calls of a hunting bat even at the start of the sweep. Responses to these high frequencies are supported by LDV recordings of tympanal motion in intact ears of free-field specimens, and behavioural audiograms that show a broad mechanical and behavioural response to ultrasounds responses (Supplementary Table S3, Fig. 5a and 5b). These broad responses to ultrasound are common in Tettigoniidae[81,82], as shown in the katydid *Neoconocephalus ensiger*, a copiphorine with ear pinnae and EC[51]. A gain of 16 – 20 dB at the start of the bat call provides essential awareness time (≤ 0.86 ms in terms of duration of the complete sweep[78]) to *C. gorgonensis* as a result of the tympanal pinnae. Other katydid species living in sympatry with *C. gorgonensis* like *Supersonus aequoreus* and *Eubliastes aethiops* exhibit similar cavity induced pressure gains in the range of phyllostomid bats (Supplementary Fig. S4).

The pressure – time difference receiver of *C. gorgonensis* is a unique system that can capture different ranges of frequencies between the multiple entry ports that can atone the limitations of each but is also capable of compensating for limitations in auditory orientation[14]. For katydids, incident sounds from elevation are difficult to perceive[33]. The ability of the external port to be positioned and rotated in accordance with the movement of the foretibial knee and foretibial leg joints permits for the ear to be more vertically oriented. The µ-CT imaging presented here of the tympanal cavities supports the theory for vertical orientation as the sub-slit cavity is asymmetrically recessed to the distal end, which is likely to enhance mechanical responses to vertical stimuli (Fig. 1d). For ultrasonic reception, a total of four asymmetrical external ports (left and right ATMs and PTMs) may be behaviourally articulated in a manner to enhance the detection of elevated bat calls, and the physical separation between the external ports of each ear yield sufficient binaural cues.

410

411 ***Katydid ear pinnae and the fossil record***

412 The presence of ear pinnae in katydids is unknown in the fossil record. Katydid ancestors (e.g.,
413 Haglidae and Prophalangopsidae from upper Jurassic[83]) and early katydids from the middle
414 Paleogene (Eocene, ~55 mya[84,85]) all show naked tympana (without pinnae). The earliest
415 echolocating bats are from the Eocene[86], therefore katydids with tympanal pinnae on their ears
416 may have initially evolved such sophisticated hearing devices to survive nocturnal predators
417 while they sing under the cover of darkness. Although katydid ear pinnae have never been
418 mapped in the most recent molecular phylogenies[87,88], we observe a potential unique origin of
419 ear pinnae in the family Tettigoniidae, with multiple losses in modern species, including the
420 large Phaneropterinae (predominantly known to have naked tympana). Comparative analyses
421 using large phylogenies are needed to solve this working hypothesis. Analogous ear pinnae
422 adaptations are observed in some Eneopterinae crickets (Tribe Lebinthini)[89], which differ from
423 field crickets in their use of high frequencies for specific communication (12-28 kHz). These
424 crickets emerged also in the Eocene[90] and while their ancestors exhibit only one functional
425 tympanum (PTM) the extant forms show two functional asymmetric tympana, with the ATM
426 covered by pinnae[89]. Such adaptation suggests a new paradigm of the dual role of the ears, in
427 detecting conspecific calls and bat echolocation.

428 Several katydid species (e.g., Phaneropterinae, Mecopodiae) exhibit naked tympana
429 (Supplementary Fig. S1b). While little is known about the ecology of many species, katydids
430 have developed diverse hearing structure morphologies to respond to predation pressure[91]. Ears
431 evolve very rapidly[4,91] and it would not be surprising that, without pinnal structures, some
432 nocturnal Phaneropterinae evolved sophisticated ECs with exceptional broadband response
433 (i.e., broader than that of *C. gorgonensis*) [16,18,41] . A study from Barro Colorado Island reported

434 31 Phaneropterinae katydids from Barro Colorado Island, of which about 42% use calling
435 songs in the low ultrasonic range while 74% showing a spectral bandwidth of > 10 kHz[92]. It
436 might also be possible that some Phaneropterinae have a unique ear function via the EC which
437 is capable of detecting conspecific calls as well as bats. This configuration of a single ear
438 function is also potentially exhibited by *Supersonus aequoreous* (Supplementary Fig. S3)
439 which show atrophied EC, and rest of the outer ear components (tympana and pinnae)
440 specialised in identifying the direction of their own calls while at the same time detecting bats.
441 Other adaptations of katydids without tympanal pinnae might involve activity during the
442 daytime[81,82], or dwell in dense vegetation that challenges flying[93]. For example, *Phlugis* and
443 *Speculophlugis* species are diurnal visual predators that need day light to hunt[94]. Owing to their
444 transparent camouflage, males are able to sing below Araceae leaves during the day and avoid
445 visual detection by diurnal avian predators. Other katydids like *Conocephalus* sp. with
446 tympanal pinnae are also active during the day time, although a few species are nocturnal or
447 crepuscular, but a majority dwell in dense grass vegetation. Their calling songs are of unusual
448 broadband energy (in many species expanding above 60 kHz[95]) and all *Conocephalus* sp. In
449 this case, the retention of the pinnal condition might be associated with specific directional
450 hearing like acoustic ranging[96] in such dense grass environments[41,97].

451 While the diversity of form and function of pinnae in katydids requires a deeper comparative
452 analysis, the presented findings suggest that in the assessed species, pinnae act as ultrasonic
453 resonators for the early detection of echolocating bats. As a working hypothesis, we propose
454 that the ear pinnae have a unique origin across the ca. 8000 species of Tettigoniidae[9] in response
455 to the emergence of bats during the early Eocene, and that it was subsequently lost several
456 times.

457

Materials and methods

Specimens

Copiphora gorgonensis (Tettigoniidae: Copiphorini) is endemic to Gorgona National Natural Park, Colombia (02°58′03″N 78°10′49″W). The original generation of the species were imported to the UK under the research permit granted by the Colombian Authority (DTS0-G-090 14/08/2014) in 2015. The specimens were ninth generation, captive bred colonies and maintained at 25°C, 70% RH, light: day 11 h: 23 h. They were fed *ad libitum* diet of bee pollen (Sevenhills, Wakefield, UK), fresh apple, dog food (Pedigree Schmackos, UK) and had access to water. Live experiments were conducted on seven adults of *C. gorgonensis* from our laboratory breeding colonies at the University of Lincoln (Lincoln, UK). Following experimentation, these specimens plus an additional four females already stored in ethanol were micro-CT scanned for finite element modelling; totalling 17 ears (10 female, 7 male). Live specimens were preserved in ethanol-filled jars and stored in a freezer at – 22°C at the University of Lincoln (Lincoln, UK).

Simultaneous recordings of tympanal vibrations using laser Doppler Vibrometry

Insects were chemically anesthetized using triethylamine-based agent FlyNap (Carolina Biological Supply, USA) for 15 min prior to the mounting process, and remained awake throughout the duration of the experiment. The animals were dorsally mounted using a specialized platform to isolate the external and internal sound inputs and also mimic their natural stance. A rosin-beeswax mix was used to fix the pronotum, and the mid and hind legs, to the mount. This specialized platform[13] consists of a two Perspex panels (1.61 mm diameter) that are joined by latex and suspended in the air by a 12 x 12 mm metal frame attached to a micromanipulator (World Precision Instruments, Inc., USA) (see[35]). At the Perspex junction,

the forelegs of the insect were extended through arm holes cut in the Perspex and attached on a rubber block with metal clasps. A metal clasp was placed on each foretibia and forefemur (total of 4) to arrest foreleg motion. The arm holes and frame borders were sealed with latex to deny sound propagation to the spiracle.

The LDV system consisted of a the OFV-2520 Dual Channel Vibrometer - range velocity controller for operating two single point laser sensor heads, sensor heads hereafter (OFV-534, Polytec, Germany) each with VIB-A–534 CAP camera video feed and laser filters. Each sensor head was mounted on a two-axis pivoting stage (XYZ, Thorlabs Inc., USA) anchored to an articulating platform (AP180, Thorlabs Inc., USA) and manually focused at 10.5 cm above a vibration isolation table (Pneumatic Vibration Isolation Table with a B120150B - Nexus Breadboard, 1200 mm x 1500 mm x 110 mm, M6 x 1.0 Mounting Holes, Thorlabs Inc., USA) supported by an anti-vibration frame (PFA52507 - 800 mm Active Isolation Frame 900 mm x 1200 mm, Thorlabs Inc., USA) in an anechoically isolated chamber (AC Acoustics, Series 120a, internal dimensions of 2.8 m x 2.7 m x 2 71 m). The sensor heads were outfitted with magnification microscopic lenses (Mitutoyo M Plan 10x objective for Polytec PSV-500 single laser head OFV 534, Japan) and positioned about 35 to 40 mm away from the insect foreleg at 45° angles towards the Perspex surface (Supplementary Fig. S5). The narrow entrance to the tympanal cavities restricted the use of LDV to measure tympanal responses across the entire tympanal membrane. Therefore, the placement of the sensor heads was limited to positions where the sensor heads were perpendicular to the tympanic membrane of interest. The sensor speeds were maintained at 0.005 (m/s)/V and recorded using an OFV-2520 internal data acquisition board (PCI-4451; National Instruments, USA).

Tympanal vibrations were induced by a four-cycle sinusoidal wave at 23, 40 and 60 kHz. The closed-field configuration of the loudspeaker restricts the delivery of high ultrasonic stimuli to 60 kHz. A rotating automated stage (PRM1Z8 rotation mount, Thorlabs Inc., USA) with a

KDC101 K-Cube™ DC Servo Motor Controller (Thorlabs Inc., USA) positioned a multi-field magnetic loudspeaker (MF1, Tucker Davis, USA) with a parabolic nozzle (see Supplementary Materials from[14]) and plastic probe tip (3.5 cm L x internal diameter 1.8 mm W) about 3.5 mm away from the mounted insect and 10.2cm above the breadboard table. The speaker was moved across a 12 cm semi-circle in 1° steps (0.56 mm). The probe tip was positioned at "point zero" and 20 single shot recordings at 1°, totalling 10° at either side of this port (Supplementary Fig. S6). A high quality 500 band pass filter was applied at 10 to 30 kHz for the 23 kHz recordings, 30 to 50 kHz for the 40 kHz recordings, and 50 to 70 kHz for the 60 kHz recordings. All acoustic signals were generated by a waveform generator (SDG 1020, Siglent, China), synchronized with the LDV, amplified (ZB1PS, Tucker Davis, USA) and measured by a 1/8″ (3.2 mm) omnidirectional microphone (Type 4138, Brüel & Kjaer, Nærum Denmark) located about 3 mm from tympanum. The microphone, with built in preamplifier (B&K 2670, Brüel & Kjær, Nærum, Denmark), was calibrated using a sound-level calibrator (Type 4237, Brüel & Kjaer, Nærum, Denmark) and set to 316 mV/Pa output via a conditioning amplifier (Nexus 2690-OS1, Brüel & Kjær, Nærum, Denmark). A reference measurement was performed by placing the microphone 3 mm from the probe tip to the loudspeaker before each experiment. Using a micro-manipulator, the microphone was positioned approximately 3 to 3.5 mm from the ear to monitor the acoustic isolation of the platform.

Experimental procedures

The sensor heads were manually focused on the external tympanal surface using the 2-axis pivoting stage and manual wheel with the aid of the sensor head camera output displayed on an LED screen. For the time measurements, the point zero was found for each leg and for each test frequency. The point zero was the point where the displacements from the anterior

tympanic membrane (ATM) and posterior tympanic membrane (PTM) matched the oscillation phase of the generated 4-cycle sinusoidal waves. This ensured that the vibrations of the tympanic membranes were synchronous relative to the speaker position. Displacement amplitudes from the same cycle order number were measured from each sensor head reference, and approximately 252 data points were measured per ear.

After recording the vibrations for both insect ears, the cuticular pinnae were carefully excised (not to damage the tympanal organs or the fine layer of tissue ventrally connected to the tympanic membranes) using a razor blade. The measurements were repeated for each ear following the same protocol.

Time and displacement measurements were analysed by identifying the second oscillation of the 4-cycle tone generated waves in each PSV software window (PSV 9.4 Presentation software, Polytec, Germany).

Morphological studies of the ear

To produce 3D data for modelling, 17 ears of *C. gorgonensis* were scanned using a SkyScan 1172 X-ray micro-CT scanner (Bruker Corporation, Billerica, MA, USA) with a resolution between 1.3 and 2.9 µm (55 kV source voltage, 180 µA source current, 300 ms exposure and 0.1° rotation steps). As experimental procedures required removal of the cuticular pinnae, eight additional specimens with intact pinnae were scanned. The micro-CT projection images were reconstructed with NRecon (v.1.6.9.18, Bruker Corporation, Billerica, MA, USA) to produce a series of orthogonal slices. The 3D segmentation of the ear, measurements of the ear cross section and width, and volumetric measurements of the cavities formed by the pinnae were performed with the software Amira-Aviso 6.7 (Thermo Fisher Scientific, Waltham,

554 Massachusetts, USA). Micro-CT stereolithography files (STL) were generated for numerical
555 modelling using established protocols[13,14] and to 3D print ear models.

556 For 2D measurements of the cavity slit area, pinnal protrusion, and the distance between the
557 pinnal cavities, an Alicona InfiniteFocus microscope (G5, Bruker Alicona Imaging, Graz,
558 Austria) at x5 objective magnification was used to capture images with a resolution of abou100
559 nm of collection specimens with pinnae intact (n = 8 ears).

560

561 ***Bat and insect call recordings***

562 The echolocation calls of phyllostomid bats (Chiroptera: Phyllostomidae) native to Gorgona
563 Island were recorded in 2015. The call of *Micronycteris megalotis* was recorded using the Echo
564 Meter Touch 2 (Wildlife Acoustics, Maynard, MA, USA), with a sampling rate of 384 kHz.
565 *Gardnerycteris crenulatum*, *Tonatia saurophila* and *Micronycteris microtis* were recorded in
566 a small indoor flight cage (1.4 x 1.0 x 0.8 m) in which they were allowed to fly via an ultrasound
567 condenser microphone (2-200 kHz frequency range, ±3 dB frequency response between 25-
568 140 kHz; CM16, CMPA preamplifier unit, Avisoft Bioacoustics, Glienicke, Germany) and real
569 time ultrasound acquisition board (6 dB gain, 500 kHz sampling rate, 16 bit resolution;
570 UltraSoundGate 116Hm, Avisoft Bioacoustics, Glienicke, Germany) connected to a laptop
571 (Think Pad X220, Lenovo, Beijing, China), with a corresponding recording software (Avisoft
572 RECORDER USGH, Avisoft Bioacoustics, Glienicke, Germany). These are the most common
573 insectivorous gleaning species in the habitat of *C. gorgonensis*. Call description of single calls
574 is presented as Supplementary Fig. S7.

575 *SI Appendix*, Section 1 (see Supplementary Fig. S8) has details of male *C. gorgonensis* calling
576 song recording.

577

Acoustics measurements of synthetic 3D-printed scaled ear models

For time domain measurements, 3D models of the ears were placed on a micromanipulator arm with blu-tac (Bostik Ltd, Stafford, UK) and positioned frontally 30 cm from a MF1 loudspeaker at the same elevation. A 25 mm tipped B&K Type 4182 probe microphone (Brüel & Kjær, Nærum, Denmark) with a 1 × 25 mm (0.99″) probe tube length and 1.24 mm (0.05″) interior diameter, calibrated using a B&K Type 4237 sound pressure calibrator was placed ventral to the ear. The ear moved onto the microphone using an electronic micromanipulator (TR10/MP-245, Sutter Instrument, Novato, California, USA), to a position 1 cm from the back of the cavity. Stimuli delivered were individually scaled to match the wavelength of a real-size ear (e.g., for a 1:10 scale printed model, the frequency delivered to simulate 120 kHz would be 120/10 = 12 kHz) to account for variation in printed model scaling. 3D printed models were scaled 1:11.43 (male 1:11.33; female 1:11.53) with the corresponding average scaled stimuli of 2.01 kHz for 23 kHz, 3.50 kHz for 40 kHz, 5.25 kHz for 60 kHz, and 9.63 kHz for 110 kHz. Four cycle pure tones were produced using the aforementioned function generator, and the amplitude set to deliver 1 Pa to the microphone at each frequency. Received signals were amplified using a B&K 1708 conditioning amplifier (Brüel & Kjær, Nærum, Denmark), and acquired using a PSV-500 internal data acquisition board at a sampling frequency of 512 kHz. The microphone remained stationary during the experiments, nor was its direct path to the speaker obstructed. Instead, the microphone entered the ear via the drilled hole, allowing the pinnae to surround the tip of the microphone. Thus, the reported sound pressure gains result solely from the cavities of the 3D model, and not the motion of the microphone. When the microphone was positioned inside the cavities, the gap between the drilled hole and microphone probe was sealed with blu-tac (Bostik Ltd, Stafford, UK) to mimic the real cavity and avoid acoustic leaking (refer to Supplementary Materials Section 2: Video 1).

602 To calculate the frequency that produced the best gain, the MF1 loudspeaker was replaced with
603 a RAAL 140-15D Flatfoil loudspeaker (RAAL, Serbia), with a different amplifier (A-400,
604 Pioneer, Kawasaki, Japan). This speaker was able to deliver a broadband stimulus of periodic
605 chirps, generated within Polytec 9.4 software, with a simulated frequency range of 2-150 kHz.
606 Recording in the frequency domain, at a sampling frequency of 512 kHz, the amplitude of the
607 broadband stimulus was mathematically corrected within the software to deliver 60 dB at all
608 frequencies. The reference frequency spectrum with no ear present could be subtracted from
609 the frequency spectrum reported within the cavities to calculate frequency-specific gain and
610 thus cavity resonance. Gain was calculated by subtracting the probe microphone sound pressure
611 (dB) measured 1 cm outside of the cavity from inside the tympanal cavity measurements (Fig.
612 3b and 3c; see also Supplementary Materials Section 2: Video 1).

613 For comparative purposes, the ears of the following sympatric and pinnae bearing katydid
614 species from Gorgona Island were also 3D printed and subjected to experiments according to
615 the aforementioned protocol: *Supersonus aequoreus*, *Eubliastes aethiops*, and Pleminiini sp.
616 (see Supplementary Fig. S3).

617 Frequency domain recordings of the cavity resonance, and time domain recordings of pure tone
618 gains were then exported as .txt files for analysis. Methods for printing 3D ear models are
619 provided in the Supplementary Materials Section 1.

620

621 ***Mathematical models and numerical simulations***

622 The mathematical models have been constructed as a scattering acoustic – structure interaction
623 problem and simulate the acoustic response of the tympanal cavities to an incident plane
624 acoustic wave in an air domain. Hence, the 3D model considers the interaction of the sound
625 wave with the ear, for which realistic material properties have been incorporated. The air

acoustic domain is truncated as a sphere with a 3 mm radius that is centered around the ear (Supplementary Fig. S9). Two different geometries of the ears were taken as part of the mathematical model domain: pinnae intact and pinnae removed (Supplementary Fig. S10).

The models were considered both in the frequency and the time domains, and were solved using the acoustic-shell interaction module of the software Comsol Multiphysics, v5.6[98]. For the frequency domain models, the incident wave was taken to be a chirp with an amplitude of 1 Pa and frequency 2-150 kHz, directed at "point zero" as defined in the in the section *vibrational measurements*. For the time domain models, three different incident waves were used, with amplitudes 1 Pa and frequencies 23, 40, 60 kHz. The direction of the waves was taken as -10°, -5°, 0°, 5° and 10° on a fixed plane perpendicular to the ear, with 0° corresponding to "point zero". The details of the solved system of equations can be found in Supplementary Materials Section 1.

The numerical solution to the problem was obtained using the finite element method for the spatial variables in both the time and frequency domain simulations. For forming the finite-element mesh, the maximum diameter used for the tetrahedral elements in the sphere was $h_{max} = \frac{c}{6 \times f_0}$, where $c = 343\ \mathrm{m/s}$ and $f_0 = 150\ \mathrm{kHz}$ (Supplementary Fig. S11 and S12). Hence, even at the largest frequency considered, there were six tetrahedral elements per wavelength. Quadratic Lagrange elements were applied for the solution.

For the time domain solution, the time variable was solved for using the Generalized alpha method, with a constant time step of $\Delta t = \frac{1}{60 \times 150}\ \mathrm{s}$, so that the Courant-Friedrichs-Lewy (CFL) condition[99], defined as $CFL = \frac{c \times h_{max}}{\Delta t}$ was 0.1, which gives a reliable approximation of the solution.

649 ***Behavioral and tympanal response to broadband stimulation***

650 Behavioral audiograms: Behavioral audiograms were performed on nine tethered female (*n* =
651 9) *C. gorgonensis* to test behavioral response thresholds to controlled auditory stimuli (20 –
652 120 kHz). Methods are provided in Supplementary Materials Section 1.

653 Tympanal tuning: We exposed seven (4 males, 3 females) specimens to free field broadband
654 (periodic chirp 20 – 120 kHz) stimulation presented by an ipsilaterally positioned SS-
655 TW100ED Super-Tweeter (Sony, Tokyo, Japan) with a 20 kHz built-in high-pass filter using
656 an Avisoft Bioacoustics Ultrasonics Power Amplifier (Avisoft Bioacoustics,
657 Glienicke/Nordbahn, Germany). A rosin-beeswax mix was used to fix the pronotum, and the
658 mid and hind legs, to the mount (see[35]) after the insects were chemically anesthetized using
659 FlyNap. Insects were then elevated to the same level as the LDV vibrometer and positioned
660 15 cm from the loudspeaker. A B&K Type 4138 microphone was placed about 3 mm in front
661 of the ear of interest and recorded the stimulus. Mechanical responses were acquired using a
662 PSV-500 internal data acquisition board at a sampling frequency of 512 kHz. The amplitude
663 was corrected to maintain 60 dB SPL at all frequencies. Data was collected as magnitude
664 (velocity / sound pressure).

665

666 ***Statistical analyses***

667 Using empirical data we tested the effect of cuticular pinnae on tympanal responses (in
668 displacement amplitude (natural log transformed) and arrival time) to incident sound, we fitted
669 linear mixed models (LMM) with angle (-10° to 10°, polynomial continuous variable) as a
670 covariate and presence of pinnae (y/n), frequency (23, 40 and 60 kHz, categorical variable),
671 tympanum (ATM or PTM) as fixed factors. We include the interactions between angle and
672 pinnae and between pinnae and frequency. To model the curvature in the response surface of

673 the pinnal enclosed tympanum, angle was fitted as a quadratic polynomial with 0° (at point
674 zero). The interaction of angle and pinnae was fitted as such to show the restriction of pinnal
675 structures in both time and displacement to the response surface. We carried out post hoc tests
676 between pinnae (y/n) at each frequency using estimated marginal means from the package
677 emmean[100].

678 To determine differences in both the anatomy and estimated resonance of the anterior and
679 posterior pinnae, we carried out two-sample *t*-test and Wilcoxon rank sum (or Mann-Whitney
680 U test) depending on data distribution. These anatomical differences included the area of the
681 entrance to the cavity, cavity volume, and protrusion.

682 Using the same initial LMM model, we tested how sound pressure estimated from numerical
683 models was related to angle (-10° to 10°, polynomial continuous variable), presence of pinnae
684 (y/n), frequency (23, 40 and 60 kHz, categorical variable), tympanum (ATM or PTM) as fixed
685 factors. Again, we include the interactions between angle and pinnae and between pinnae and
686 frequency. We finally tested sound pressure based on 3D models. the presence of pinnae (y/n),
687 frequency (23, 40 and 60 kHz, categorical variable), tympanum (ATM or PTM) as fixed
688 factors, with the inclusion of the interaction between pinnae and frequency. For both numerical
689 and 3D models, we carried out post hoc tests between pinnae (y/n) at each frequency using
690 estimated marginal means from the package emmeans.

691 All LMMs were run using the package lmerTest[101] in R 4.0.0[102]. Statistical tests and graphs
692 were performed on R 4.0.0[102].

693

694 ***Data availability***

695 Experimental data (LDV recordings), numerical simulations, Comsol model files, and µ-CT
696 stereolithography files (in .stl format) are available in Dryad
697 (https://doi.org/10.5061/dryad.k0p2ngf8x).

698

699 **Acknowledgements**

700 We thank the Orthopterists' Society for aiding in funding the micro-CT work of CW, for which
701 some data has been used in this study, and to the University of Lincoln's School of Life
702 Sciences for CW's PhD studentship.

703

704 **Author contributions**

705 All authors were involved in writing and revision of the manuscript. CP and FM-Z performed
706 acoustic experiments on live specimens. CP and CW designed and performed all 3D print
707 model experiments. CP constructed the speaker mount, automated the controls in the arena,
708 collected and analysed data. CS designed the statistical model and completed statistical
709 analyses. EC developed and performed all numerical models and simulations. CW illustrated
710 figures, conducted µ-CT scans, performed all post-image segmentation for numerical analyses,
711 and conducted 3D printing. IG and FM-Z recorded insect and bat acoustic signals. FM-Z and
712 DC performed behavioural audiograms. FM-Z and CP conceived the idea for the project. FM-
713 Z led the lab, assisted with idea development, and provided equipment training.

714

715 **Competing interests**

716 No competing interests declared

Funding

This research is part of the project "The Insect Cochlea" funded by the European Research Council, Grant ERCCoG-2017-773067 to FM-Z; and was also funded by the Natural Environment Research Council (NERC), grant DEB-1937815 to FM-Z.

References

1. Göpfert, M. C. & Hennig, R. M. Hearing in Insects. *Annu. Rev. Entomol.* **61**, 257–276 (2016).
2. Robert, D. Directional Hearing in Insects. in *Sound Source Localization* (eds. Popper, A. N. & Fay, R. R.) 6–35 (Springer New York, 2005). doi:10.1007/0-387-28863-5_2.
3. Warren, B. & Nowotny, M. Bridging the Gap Between Mammal and Insect Ears – A Comparative and Evolutionary View of Sound-Reception . *Frontiers in Ecology and Evolution* vol. 9 504 (2021).
4. Song, H. *et al.* Phylogenomic analysis sheds light on the evolutionary pathways towards acoustic communication in Orthoptera. *Nat. Commun.* **11**, 4939 (2020).
5. Strauß, J. & Stumpner, A. Selective forces on origin, adaptation and reduction of tympanal ears in insects. *J. Comp. Physiol. A* **201**, 155–169 (2015).
6. Lakes-Harlan, R. & Scherberich, J. Position-dependent hearing in three species of bushcrickets (Tettigoniidae, Orthoptera). *R. Soc. Open Sci.* **2**, 140473 (2015).
7. Suga, N. Principles of auditory information-processing derived from neuroethology. *J. Exp. Biol.* **146**, 277–286 (1989).
8. Hartbauer, M. & Römer, H. From microseconds to seconds and minutes-time

computation in insect hearing. *Front. Physiol.* **5 APR**, 1–12 (2014).

9. Cigliano, M. M., Braun, H., Eades, D. C. & Otte, D. Orthoptera Species file v.5.0. *Orthoptera Species File* http://orthoptera.speciesfile.org (2021).

10. Bailey, W. J. The ear of the bushcricket. in *The Tettigoniidae. Biology, systematics and evolution* (eds. Bailey, W. J. & Rentz, D.) 217–247 (Crawford House Press, 1990).

11. Strauß, J., Lehmann, A. W. & Lehmann, G. U. C. Sensory evolution of hearing in tettigoniids with differing communication systems. *J. Evol. Biol.* **27**, 200–213 (2014).

12. Kalmring, K. *et al.* The Auditory-Vibratory Sensory System in Bushcrickets (Tettigoniidae, Ensifera, Orthoptera) I Comparison of Morphology, Development and Physiology. in *Environmental Signal Processing and Adaptation* (eds. Heldmaier, G. & Werner, D.) 169–207 (Springer Berlin Heidelberg, 2003). doi:10.1007/978-3-642-56096-5_9.

13. Jonsson, T., Montealegre-Z, F., Soulsbury, C. D., Robson Brown, K. A. & Robert, D. Auditory mechanics in a bush-cricket: direct evidence of dual sound inputs in the pressure difference receiver. *J. R. Soc. Interface* **13**, 20160560 (2016).

14. Veitch, D. *et al.* A narrow ear canal reduces sound velocity to create additional acoustic inputs in a microscale insect ear. *Proc. Natl. Acad. Sci. U. S. A.* **118**, (2021).

15. Lewis, B. the Physiology of the Tettigoniid Ear. *Methods* 861–869 (1974).

16. Michelsen, A. & Larsen, O. N. Biophysics of the ensiferan ear - I. Tympanal vibrations in bushcrickets (Tettigoniidae) studied with laser vibrometry. *J. Comp. Physiol. A* **123**, 193–203 (1978).

17. Nocke, H. Physical and physiological properties of the tettigoniid (‘grasshopper’) ear. *J. Comp. Physiol. A* **100**, 25–57 (1975).

762 18. Hoffmann, E. & Jatho, M. The acoustic trachea of Tettigoniids as an exponential horn:
763 Theoretical calculations and bioacoustical measurements. *J. Acoust. Soc. Am.* **98**,
764 1845–1851 (1995).

765 19. Larsen, O. N. Mechanical time resolution in some insect ears - II. Impulse sound
766 transmission in acoustic tracheal tubes. *J. Comp. Physiol. A* **143**, 297–304 (1981).

767 20. Michelsen, A., Rohrseitz, K., Heller, K. G. & Stumpner, A. A new biophysical method
768 to determine the gain of the acoustic trachea in bushcrickets. *J. Comp. Physiol. A* **175**,
769 145–151 (1994).

770 21. Michelsen, A. & Larsen, O. N. Pressure difference receiving ears. *Bioinspiration and*
771 *Biomimetics* **3**, 011001 (2008).

772 22. Autrum, H. Über Lautäusserungen und Schallwahrnehmung bei Arthropoden II. *Z.*
773 *Vgl. Physiol.* **28**, 326–352 (1940).

774 23. Autrum, H. Anatomy and physiology of sound receptors in invertebrates. *Acoust.*
775 *Behav. Anim.* 412–433 (1963).

776 24. Bailey, W. J. & Stephen, R. O. Directionality and auditory slit function: A theory of
777 hearing in bushcrickets. *Science (80-.).* **201**, 633–634 (1978).

778 25. Stephen, R. O. & Bailey, W. J. Bioacoustics of the ear of the bushcricket Hemisaga
779 (Sagenae). *J. Acoust. Soc. Am.* **72**, 13–25 (1982).

780 26. Mason, A. C., Morris, G. K. & Wall, P. High ultrasonic hearing and tympanal slit
781 function in rainforest katydids. *Naturwissenschaften* **78**, 365–367 (1991).

782 27. Shen, J. A peripheral mechanism for auditory directionality in the bushcricket
783 Gampsocleis gratiosa: Acoustic tracheal system. *J. Acoust. Soc. Am.* **94**, 1211–1217
784 (1993).

785 28. Michelsen, A. & Nocke, H. Biophysical Aspects of Sound Communication in Insects.
786 *Adv. In Insect Phys.* **10**, 247–296 (1974).

787 29. Eisner, N. & Popov, A. V. Neuroethology of Acoustic Communication. in vol. 3683
788 229–355 (1978).

789 30. Hill, K. G. & Oldfield, B. P. Auditory function in tettigoniidae (Orthoptera:Ensifera).
790 *J. Comp. Physiol. A* **142**, 169–180 (1981).

791 31. Yack, J. E. The structure and function of auditory chordotonal organs in insects.
792 *Microsc. Res. Tech.* **63**, 315–337 (2004).

793 32. Montealegre-Z, F. & Robert, D. Biomechanics of hearing in katydids. *J. Comp.*
794 *Physiol. A Neuroethol. Sensory, Neural, Behav. Physiol.* **201**, 5–18 (2015).

795 33. Römer, H. Directional hearing in insects: biophysical, physiological and ecological
796 challenges. *J. Exp. Biol.* **223**, Pt 14 (2020).

797 34. Montealegre-Z, F. & Postles, M. Resonant sound production in Copiphora gorgonensis
798 (Tettigoniidae: Copiphorini), an endemic species from Parque Nacional Natural
799 Gorgona, Colombia. *J. Orthoptera Res.* **19**, 347–355 (2010).

800 35. Montealegre-Z, F., Jonsson, T., Robson Brown, K. A., Postles, M. & Robert, D.
801 Convergent evolution between insect and mammalian audition. *Science (80-.).* **338**,
802 968–97 (2012).

803 36. Rossing, T. D. & Fletcher, N. H. *Principles of Vibration and Sound*. (Springer New
804 York, 2004). doi:10.1007/978-1-4757-3822-3.

805 37. Celiker, E., Jonsson, T. & Montealegre-Z, F. On the tympanic membrane impedance
806 of the katydid Copiphora gorgonensis (Insecta: Orthoptera: Tettigoniidae) . *J. Acoust.*
807 *Soc. Am.* **148**, 1952–1960 (2020).

808 38. Hummel, J., Wolf, K., Kössl, M. & Nowotny, M. Processing of simple and complex
809 acoustic signals in a tonotopically organized ear. *Proc. R. Soc. B Biol. Sci.* **281**,
810 20141872 (2014).

811 39. Windmill, J. F. C., Fullard, J. H. & Robert, D. Mechanics of a `simple' ear: tympanal
812 vibrations in noctuid moths. *J. Exp. Biol.* **210**, 2637–2648 (2007).

813 40. Bialek, W. Physical limits to sensation and perception. *Annu. Rev. Biophys. Biophys.*
814 *Chem.* **16**, 455–478 (1987).

815 41. Rheinlaender, J. & Römer, H. Insect hearing in the field. *J. Comp. Physiol. A* **158**,
816 647–651 (1986).

817 42. Windmill, J. F. C., Jackson, J. C., Tuck, E. J. & Robert, D. Keeping up with bats:
818 dynamic auditory tuning in a moth. *Curr. Biol.* **16**, 2418–2423 (2006).

819 43. Fullard, J. H. External auditory structures in two species of neotropical notodontid
820 moths. *J. Comp. Physiol. A* **155**, 625–632 (1984).

821 44. Heinrich, R., Jatho, M. & Kalmring, K. Acoustic transmission characteristics of the
822 tympanal tracheae of bushcrickets (Tettigoniidae). II: Comparative studies of the
823 tracheae of seven species. *J. Acoust. Soc. Am.* **93**, 3481–3489 (1993).

824 45. Bailey, W. J., Stephen, R. O. & Yeoh, P. Signal transmission in noisy environments:
825 Auditory masking in the tympanic nerve of the bushcricket Metaballus litus
826 (Orthoptera: Tettigoniinae). *J. Acoust. Soc. Am.* **83**, 1828–1832 (1988).

827 46. Celiker, E., Jonsson, T. & Montealegre-Z, F. The auditory mechanics of the outer ear
828 of the bush cricket: a numerical approach. *Biophys. J.* **118**, 464–475 (2020).

829 47. Fullard, J. H. Acoustic relationships between tympanate moths and the Hawaiian hoary
830 bat (Lasiurus cinereus semotus). *J. Comp. Physiol. A* **155**, 795–801 (1984).

831 48. Sarria-S, F. A., Chivers, B. D., Soulsbury, C. D. & Montealegre-Z, F. Non-invasive
832 biophysical measurement of travelling waves in the insect inner ear. *R. Soc. Open Sci.*
833 **4**, 1–11 (2017).

834 49. Bailey, W. J. The tettigoniid (Orthoptera : Tettigoniidae) ear: Multiple functions and
835 structural diversity. *Int. J. Insect Morphol. Embryol.* **22**, 185–205 (1993).

836 50. Rajaraman, K. *et al.* Low-pass filters and differential tympanal tuning in a
837 paleotropical bushcricket with an unusually low frequency call. *J. Exp. Biol.* **216**, 777–
838 787 (2013).

839 51. Faure, P. A. & Hoy, R. R. The sounds of silence: cessation of singing and song
840 pausing are ultrasound-induced acoustic startle behaviors in the katydid
841 Neoconocephalus ensiger (Orthoptera; Tettigoniidae). *J. Comp. Physiol. A* **186**, 129–
842 142 (2000).

843 52. Arlettaz, R., Ruedi, M. & Hausser, J. Ecologie trophique de deux espèces jumelles et
844 sympatriques de chauves-souris: Myotis myotis et Myotis blythii (Chiroptera :
845 Vespertilionidae). Premiers résultats: **57**, 519–532 (1993).

846 53. LaVal, R. K. & LaVal, M. L. Prey selection by the slit-faced bat Nycteris thebaica
847 (Chiroptera: Nycteridae) in Natal, South Africa. *Biotropica* **12**, 241–246 (1980).

848 54. Davison, G. & Zubaid, A. Food habits of the Lesser false vampire, Megaderma
849 spasma, from Kuala Lompat, Peninsular Malaysia. *Z. Säugetierkd.* **57**, 310–312
850 (1992).

851 55. Fenton, M. B. & Museum., R. O. *Observations on the biology of some Rhodesian*
852 *bats : including a key to the Chiroptera of Rhodesia*. (Royal Ontario Museum, 1975).

853 56. Whitaker, J. O. & Black, H. Food habits of cave bats from Zambia, Africa. *J. Mammal.*

57, 199–204 (1976).

57. Raghuram, H., Deb, R., Nandi, D. & Balakrishnan, R. Silent katydid females are at higher risk of bat predation than acoustically signalling katydid males. *Proc. R. Soc. B Biol. Sci.* **282**, 20142319 (2015).

58. Zhang, L. *et al.* Diet of Flat-Headed Bats, Tylonycteris pachypus and T. robustula, in Guangxi, South China. *J. Mammal.* **86**, 61–66 (2005).

59. Buchler, E. R. & Childs, S. B. Orientation to distant sounds by foraging big brown bats (Eptesicus fuscus). *Anim. Behav.* **29**, 428–432 (1981).

60. Murillo G, O. E., Bedoya, M. J., Velandia-Perilla, J. H. & Yusti-Muñoz, A. P. Riqueza de especies, nuevos registros y actualización del listado taxonómico de la comunidad de murciélagos del Parque Nacional Natural Gorgona, Colombia . *Revista de Biología Tropical* vol. 62 407–417 (2014).

61. Belwood, J. J. & Morris, G. K. Bat predation and its influence on calling behavior in neotropical katydids. *Science (80-.).* **238**, 64–67 (1987).

62. Belwood, J. J. Anti-Predator Defences and Ecology of Neotropical Forest Katydids, Especially the Pseudophyllinae. in *The Tettigoniidae. Biology, systematics and evolution* (eds. Bailey, W. J. & Rentz, D.) 8–26 (Springer-Verlag, 1990).

63. Nickle, D. A. & Castner, J. L. Strategies utilized by katydids (Orthoptera: Tettigoniidae) against diurnal predators in rainforests of northeastern Peru. *J. Orthoptera Res.* **4**, 75 (1995).

64. ter Hofstede, H., Kalko, E. K. V & Fullard, J. H. Auditory-based defence against gleaning bats in neotropical katydids (Orthoptera: Tettigoniidae). *J. Comp. Physiol. A. Neuroethol. Sens. Neural. Behav. Physiol.* **196**, 349–358 (2010).

877 65. ter Hofstede, H. *et al.* Revisiting adaptations of neotropical katydids (Orthoptera:
878 Tettigoniidae) to gleaning bat predation. *Neotrop. Biodivers.* **3**, 41–49 (2017).

879 66. Montealegre-Z, F., Sarria, F. A., Pimienta, M. C. & Mason, A. C. Lack of correlation
880 between vertical distribution and carrier frequency, and preference for open spaces in
881 arboreal katydids that use extreme ultrasound, in Gorgona, Colombia (Orthoptera:
882 Tettigoniidae). *Rev. Biol. Trop.* **62**, 289 (2014).

883 67. Wiley, R. H. & Richards, D. G. Physical constraints on acoustic communication in the
884 atmosphere: Implications for the evolution of animal vocalizations. *Behav. Ecol.*
885 *Sociobiol.* **3**, 69–94 (1978).

886 68. Römer, H. Environmental and biological constraints for the evolution of long-range
887 signalling and hearing in acoustic insects. *Philos. Trans. R. Soc. London. Ser. B Biol.*
888 *Sci.* **340**, 179–185 (1993).

889 69. Rentz, D. C. Two new katydids of the genus Melanonotus (Melanonotus powellorum)
890 from Costa Rica with comments on their life history strategies (Tettigoniidae:
891 Pseudophyllinae). *Entomol. News* (1975).

892 70. Morris, G. K. & Beier, M. Song Structure and Description of Some Costa Rican
893 Katydids (Orthoptera : Tettigoniidae) Author (s): Glenn K . Morris and Max Beier
894 Source : Transactions of the American Entomological Society (1890-) , Mar . - Jun .,
895 1982 , Published by : American E. **108**, 287–314 (1982).

896 71. Morris, G. K., Mason, A. C., Wall, P. & Belwood, J. J. High ultrasonic and tremulation
897 signals in neotropical katydids (Orthoptera: Tettigoniidae). *J. Zool.* **233**, 129–163
898 (1994).

899 72. Heller, K. G. Acoustic signalling in palaeotropical bushcrickets (Orthoptera:

Tettigonioidea: Pseudophyllidae): does predation pressure by eavesdropping enemies differ in the Palaeo- and Neotropics? *J. Zool.* **237**, 469–485 (1995).

73. Robinson, D. J. & Hall, M. J. Sound signalling in orthoptera. *Adv. In Insect Phys.* **29**, 151–278 (2002).

74. Geipel, I. *et al.* Bats actively use leaves as specular reflectors to detect acoustically camouflaged prey. *Curr. Biol.* **29**, 2731-2736.e3 (2019).

75. Geipel, I. *et al.* Predation risks of signalling and searching: Bats prefer moving katydids. *Biol. Lett.* **16**, 3–7 (2020).

76. Page, R. & Bernal, X. E. The challenge of detecting prey: Private and social information use in predatory bats. *Funct. Ecol.* **34**, 344–363 (2020).

77. Falk, J. J. *et al.* Sensory-based niche partitioning in a multiple predator-multiple prey community. *Proc. R. Soc. B Biol. Sci.* **282**, (2015).

78. Geipel, I., Lattenkamp, E. Z., Dixon, M. M., Wiegrebe, L. & Page, R. A. Hearing sensitivity: An underlying mechanism for niche differentiation in gleaning bats. *Proc. Natl. Acad. Sci. U. S. A.* **118**, (2021).

79. Geipel, I., Jung, K. & Kalko, E. K. V. Perception of silent and motionless prey on vegetation by echolocation in the gleaning bat Micronycteris microtis. *Proc. R. Soc. B Biol. Sci.* **280**, (2013).

80. Yoh, N., Syme, P., Rocha, R., Meyer, C. F. J. & López-Baucells, A. Echolocation of Central Amazonian 'whispering' phyllostomid bats: call design and interspecific variation. *Mammal Res.* **65**, 583–597 (2020).

81. Schul, J. & Patterson, A. C. What determines the tuning of hearing organs and the frequency of calls? A comparative study in the katydid genus Neoconocephalus

(Orthoptera, Tettigoniidae). *J. Exp. Biol.* **206**, 141–152 (2003).

82. Deily, J. A. & Schul, J. Spectral selectivity during phonotaxis: A comparative study in Neoconocephalus (Orthoptera: Tettigoniidae). *J. Exp. Biol.* **209**, 1757–1764 (2006).

83. Plotnick, R. O. Y. E. & Smith, D. M. Exceptionally preserved fossil insect ears from the Eocene Green River formation of Colorado. *J. Paleontol.* **86**, 19–24 (2012).

84. Greenwalt, D. E. & Rust, J. E. S. A new species of Pseudotettigonia Zeuner (Orthoptera: Tettigoniidae) with an intact stridulatory field and reexamination of the subfamily Pseudotettigoniinae. *Syst. Entomol.* **39**, 256–263 (2014).

85. Rust, J., Stumpner, A. & Gottwald, J. Singing and hearing in a Tertiary bushcricket. *Nature* **399**, 650 (1999).

86. Teeling, E. C. *et al.* A Molecular Phylogeny for Bats Illuminates Biogeography and the Fossil Record. *Science (80-.).* **307**, 580 LP – 584 (2005).

87. Mugleston, J. D., Song, H. & Whiting, M. F. A century of paraphyly: a molecular phylogeny of katydids (Orthoptera: Tettigoniidae) supports multiple origins of leaf-like wings. *Mol. Phylogenet. Evol.* **69**, 1120–1134 (2013).

88. Mugleston, J. D., Naegle, M., Song, H. & Whiting, M. F. A Comprehensive Phylogeny of Tettigoniidae (Orthoptera: Ensifera) Reveals Extensive Ecomorph Convergence and Widespread Taxonomic Incongruence. *Insect Syst. Divers.* **2**, (2018).

89. Schneider, E. S., Römer, H., Robillard, T. & Schmidt, A. K. D. Hearing with exceptionally thin tympana: Ear morphology and tympanal membrane vibrations in eneopterine crickets. *Sci. Rep.* **7**, 1–12 (2017).

90. Vicente, N. *et al.* In and out of the Neotropics: historical biogeography of Eneopterinae crickets. *J. Biogeogr.* **44**, 2199–2210 (2017).

946 91. Hoy, R. R. The Evolution of Hearing in Insects as an Adaptation to Predation from
947 Bats BT - The Evolutionary Biology of Hearing. in (eds. Webster, D. B., Popper, A.
948 N. & Fay, R. R.) 115–129 (Springer New York, 1992). doi:10.1007/978-1-4612-2784-
949 7_8.

950 92. ter Hofstede, H. M. *et al.* Calling songs of Neotropical katydids (Orthoptera:
951 Tettigoniidae) from Panama. *J. Orthoptera Res.* **29**, 137–201 (2020).

952 93. Lang, A. B. & Römer, H. Roost site selection and site fidelity in the neotropical
953 katydid Docidocercus gigliotosi (Tettigoniidae). *Biotropica* **40**, 183–189 (2008).

954 94. Woodrow, C., Pulver, C., Veitch, D. & Montealegre-Z, F. Bioacoustic and biophysical
955 analysis of a newly described highly transparent genus of predatory katydids from the
956 Andean cloud forest (Orthoptera: Tettigoniidae: Meconematinae: Phlugidini).
957 *Bioacoustics* **30**, 93–109 (2019).

958 95. Fullard, J. H., Morris, G. K. & Mason, A. C. Auditory processing in the black-sided
959 meadow katydidConocephalus nigropleurum (Orthoptera: Tettigoniidae). *J. Comp.*
960 *Physiol. A* **164**, 501–512 (1989).

961 96. Harness, N. C. E. & Campbell, T. Acoustic ranging in meadow katydids: female
962 preference for attenuated calls. *Bioacoustics* 1–10 (2021)
963 doi:10.1080/09524622.2021.1879681.

964 97. Romer, H. & Lewald, J. High-frequency sound transmission in natural habitats:
965 implications for the evolution of insect acoustic communication. *Behav. Ecol.*
966 *Sociobiol.* **29**, 437–444 (1992).

967 98. Comsol. COMSOL Multiphysics. www.comsol.com.

968 99. Courant, R., Friedrichs, K. & Lewy, H. On the Partial Difference Equations of

969 Mathematical Physics. *IBM J. Res. Dev.* **11**, 215–234 (1967).

970 100. Lenth, R. & Lenth, M. R. Package 'lsmeans'. *Am. Stat.* **34**, 216–221 (2018).

971 101. Kuznetsova, A., Brockhoff, P. B. & Christensen, R. H. B. lmerTest Package: Tests in
972 Linear Mixed Effects Models. *J. Stat. Software; Vol 1, Issue 13* (2017).

973 102. Team, R. C. R: A language and environment for statistical computing. (2021).

974

975 **Figure legends**

976 **Figure 1.** The ear of *Copiphora gorgonensis.* **a.** Location of the ear in the foreleg, external
977 auditory input of *Copiphora gorgonensis*. **b.** 3D anatomy of the ear, with pinnae present; **c**. 3D
978 anatomy of the following pinnae ablation, with the volume of the subslit cavities exhibited
979 (light blue); **d**. 3D model of only the subslit cavities.

980

981 **Figure 2.** The effect of pinnae in the time domain and numerical simulations. **a**. Time plots
982 from five incidence angles for the 60 kHz test sound illustrating changes in oscillation phase
983 between the anterior (ATM) and posterior (PTM) tympana of the same ear. An anatomical
984 cross section of the ear is shown with each tympanum (ATM and PTM), auditory vesicle (AV),
985 posterior and anterior bifurcated tracheal branches (PT and AT), haemolymph channel (HC)
986 and posterior and anterior pinnal structures (PP and AP). **b**. Mean arrival times (ms) of
987 presented stimuli of 23, 40 and 60 kHz with and without the pinnae from time domain
988 recordings of live experimental specimens (n = 9 ears; df = 1711). **c**. Mean displacement
989 amplitudes (nm) of the tympanic membranes for each tested frequency (23, 40 and 60 kHz)
990 with and without the presence of cuticular pinnae (*n* = 9 ears; df = 1711).. **d**. Cavity induced
991 pressure gains (with pinnae) compared to sound pressure (dB) predictions with the pinnae

992 ablated from mathematical numerical models (17 ears; 10 females, 7 males). **e**. Simulated
993 arrival times (ms) of selected frequencies (23, 40 and 60 kHz) using Comsol Multiphysics,
994 v.5.6 (17 ears; 10 females, 7 males). For means comparison plots (**b** – **e**), significance symbols
995 from post hoc analyses: '***' 0.001 '**' 0.01 '*' 0.05 'ns' 0.1 ' ' 1. Red bars with cuticular
996 pinnae and blue bars without cuticular pinnae.

997

998 **Figure 3.** Acoustic experiments with 3D printed scaled ear models. **a**. Sound pressure gains
999 (dB SPL) of 3D printed ears calculated from scaled time domain recordings for 23, 40, 60 and
1000 110 kHz. Photos of 3D printed ear models with pinnae present (**b**) and ablated (**c**) and probe
1001 microphone placement.

1002

1003 **Figure 4.** Panels **a**, **c**, and **e** depict cavity induced sound pressure distribution and gains with
1004 pinnae, panels **b**, **d**, and **f** represent sound pressure gains without the pinnae. **a** and **b**. Cross –
1005 section of the ear of *Copiphora gorgonensis* with the pinnal structures intact (**a**) and ablated
1006 (**b**). Sound pressure intensities depicted with colours for simulations of 23, 40, 60 and 110
1007 kHz. Low sound pressure dB (blue) to high sound pressure dB (red) distributions inside and
1008 outside the cavities. **c** and **d** are plots of simulated sound pressure gains (dB SPL) in the
1009 frequency ranges of 20 – 150 kHz for each tympanum. **e** and **f** are plots of relative dB gain of
1010 the tympanal cavities in the 3D printed ears. ATM in red bars and PTM in blue bars.

1011

1012 **Figure 5.** Tympanal tuning and behaviorial audiograms of *Copiphora gorgonensis***. a.**
1013 Vibrational responses to broadband chirps (20 – 120 kHz) of real tympanal membranes (n = 7;
1014 14 ears; 4 males and 3 females) of live *Copiphora gorgonensis*. Maxima resonance peaks at
1015 near calling song frequency (23 kHz) and at 107.5 kHz. Blue bar for PTM and red bar for ATM.

b. Black outline with grey shadow indicate the behavioural audiogram of ultrasound response in nine female *C. gorgonensis* during waking, with auditory threshold scale in the right. Black outline shows mean vector of SLP response at a particular frequency, shaded area represents the standard deviation across measured SPL for each.

Figure 6. Ecological relevance of pinnae in *Copiphora gorgonensis*. Sound pressure level gains (left) induced by the pinnae are present only at frequencies above c.a. 60 kHz, covering the range of echolocation frequencies of five native insectivorous gleaning bat species. The conspecific call of *C. gorgonensis* on the other hand (dB_{peak} at 23 kHz), is not enhanced by the presence of the pinnae (dB loss). Dotted line indicates the frequency at which gain = 0 dB. Spectrogram parameters: FFT size 512, Hamming window, 50% overlap; frequency resolution: 512 Hz, temporal resolution: 0.078 ms.

1038 **Figures**

1039 **Figure 1**

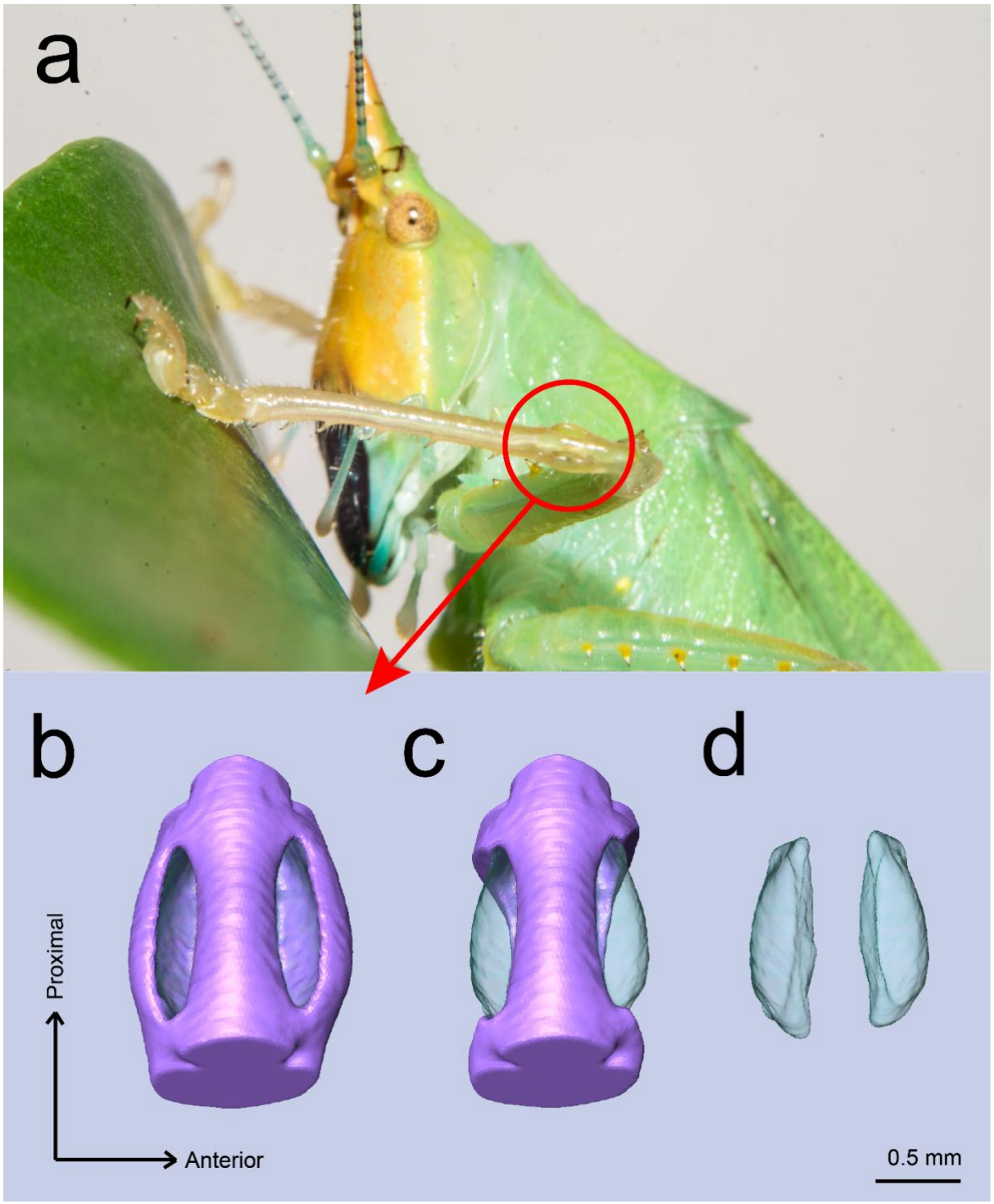

1040

1041

1042

1043 **Figure 2**

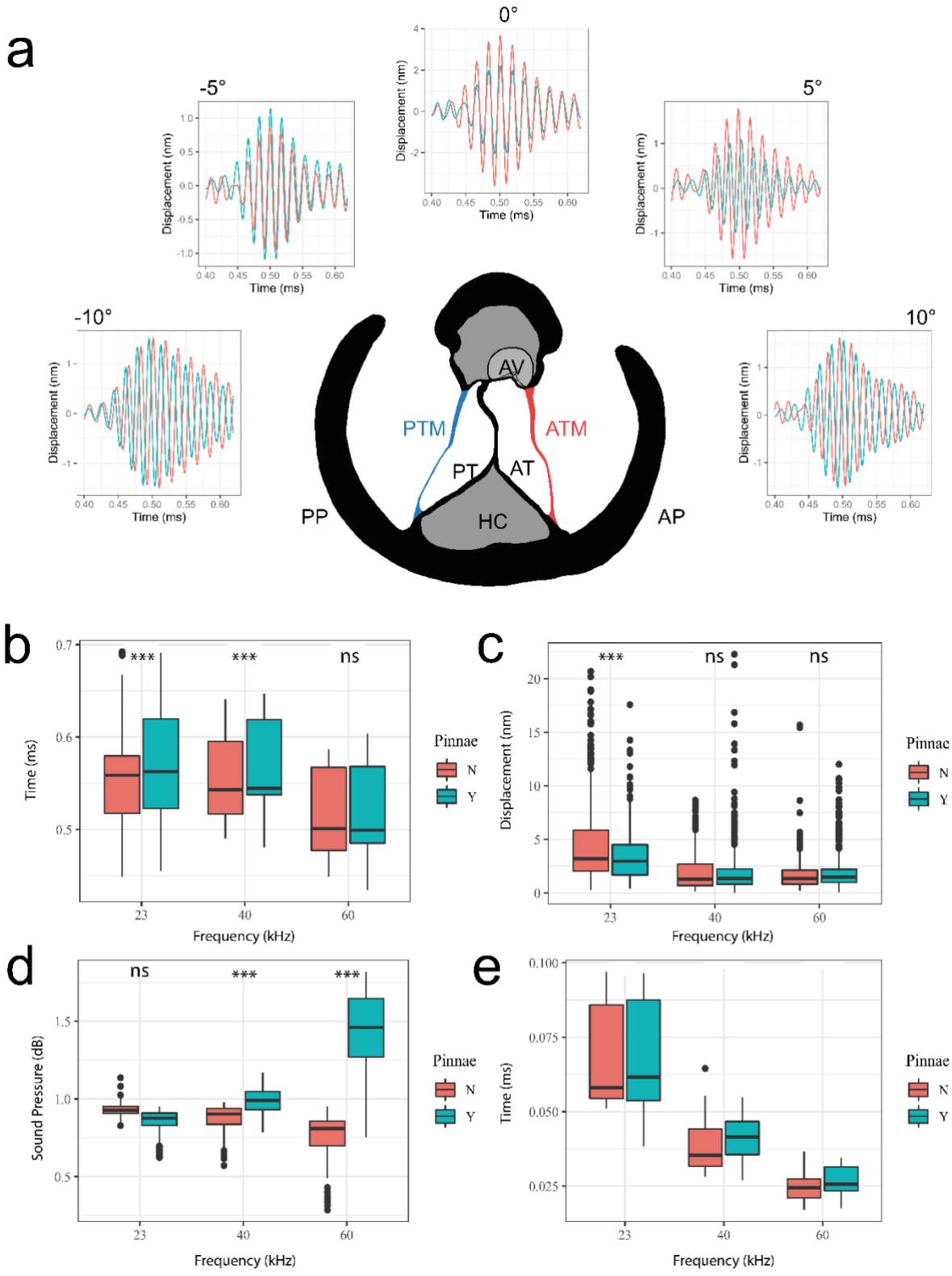

1044

1045

1046

1047 **Figure 3**

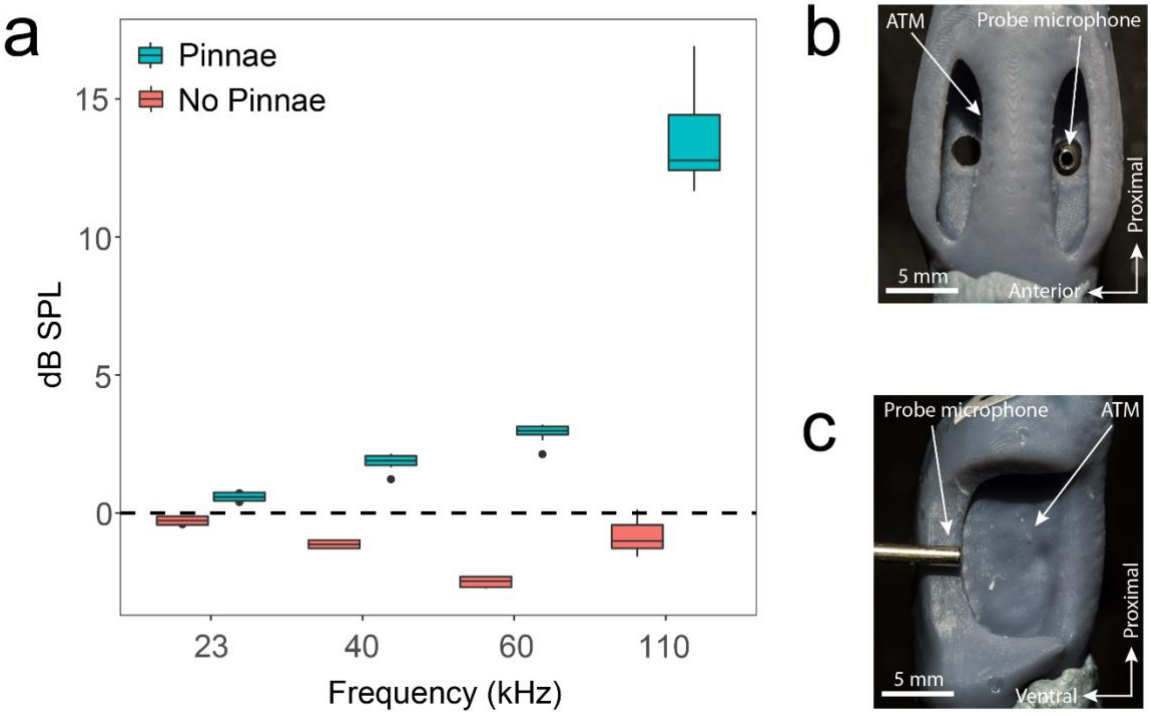

1048

1049

1050

1051

1052

1053

1054

1055

1056

1057

Figure 4

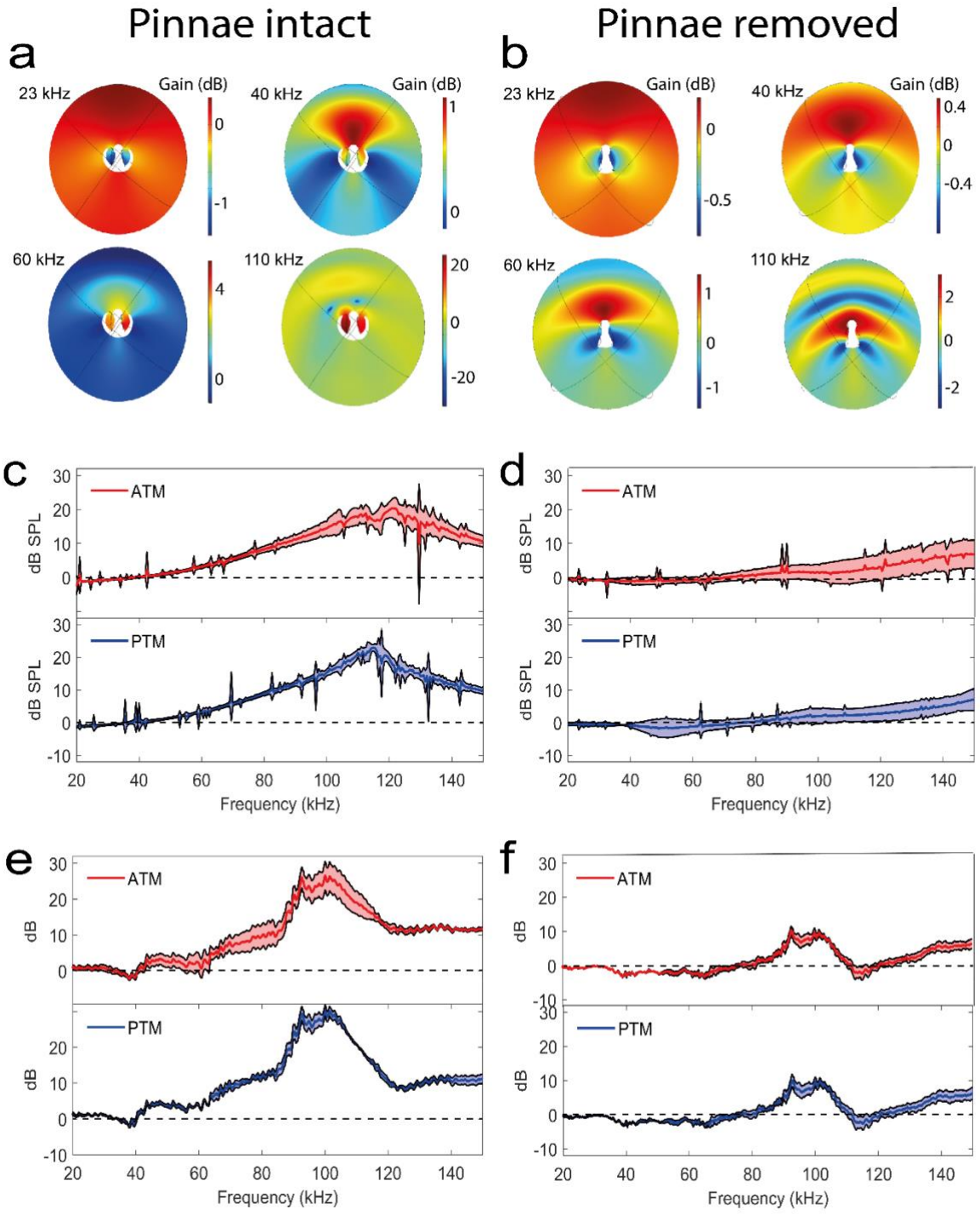

Figure 5

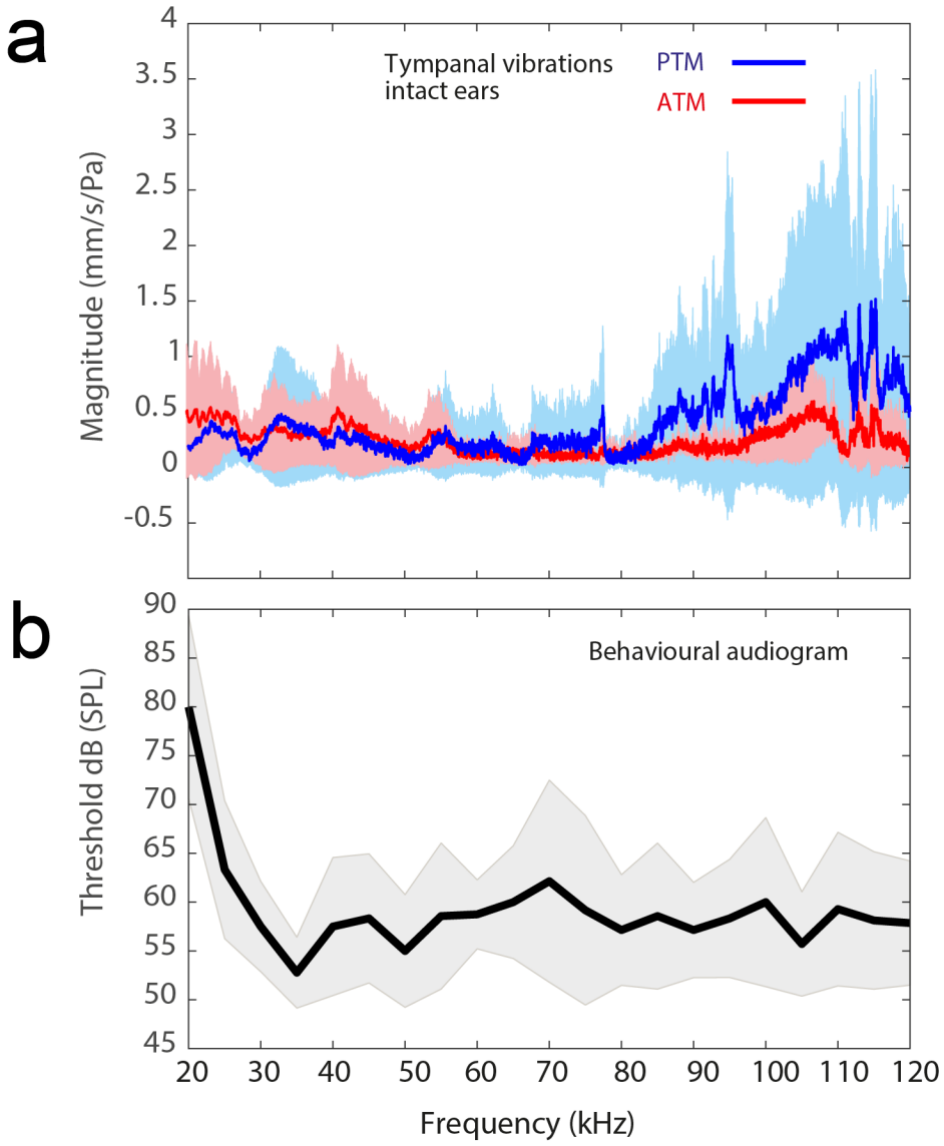

1070 **Figure 6**

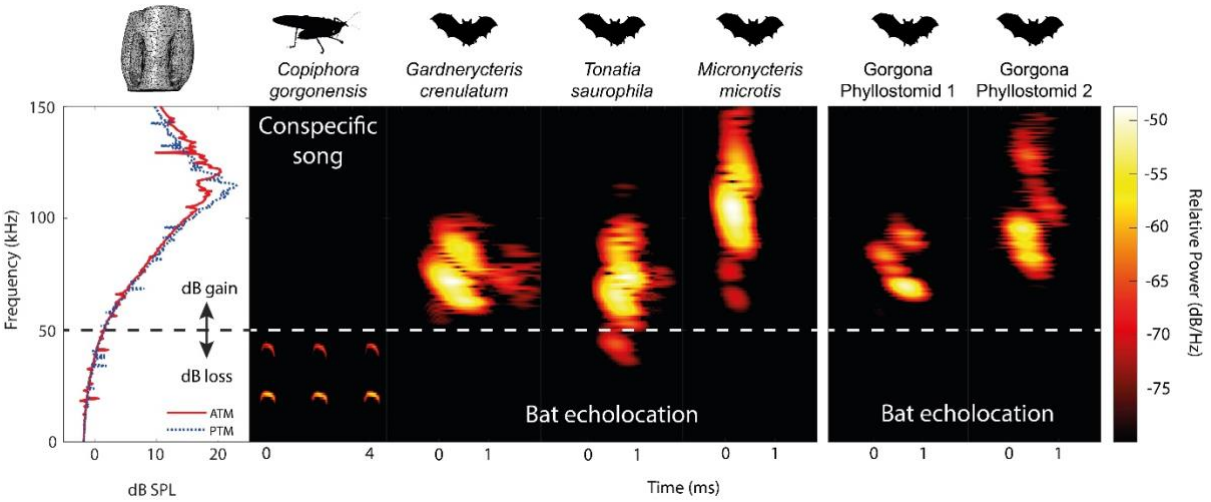

1071

1072

1073

1074

1075

1076

1077

1078

1079

1080

1081

1082

1083

1084